Constraints on extragalactic transmitters via Breakthrough Listen observations of background sources

M.A. Garrett[1,2] and A.P.V. Siemion[3,4,1]

[1]*Jodrell Bank Centre for Astrophysics (JBCA), Department of Physics & Astronomy, Alan Turing Building, The University of Manchester, M13 9PL, UK*
[2]*Leiden Observatory, Leiden University, PO Box 9513, 2300 RA Leiden, The Netherlands*
[3]*Berkeley SETI Research Center, University of California Berkeley, Berkeley CA 94720, USA*
[4]*SETI Institute, Mountain View, CA 94043, USA*

ABSTRACT

The Breakthrough Listen Initiative has embarked on a comprehensive SETI survey of nearby stars in the Milky Way that is vastly superior to previous efforts as measured by a wide range of different metrics. SETI surveys traditionally ignore the fact that they are sensitive to many background objects, in addition to the foreground target star. In order to better appreciate and exploit the presence of extragalactic objects in the field of view, the Aladin sky atlas and NED were employed to make a rudimentary census of extragalactic objects that were serendipitously observed with the 100-m Greenbank telescope observing at 1.1-1.9 GHz. For 469 target fields (assuming a FWHM radial field-of-view of 4.2 arcminutes), NED identified a grand total of 143024 extragalactic objects, including various astrophysical exotica e.g. AGN of various type, radio galaxies, interacting galaxies, and one confirmed gravitational lens system. Several nearby galaxies, galaxy groups and galaxy clusters are identified, permitting the parameter space probed by SETI surveys to be significantly extended. Constraints are placed on the luminosity function of potential extraterrestrial transmitters assuming it follows a simple power-law and limits on the prevalence of very powerful extraterrestrial transmitters associated with these vast stellar systems are also determined. It is demonstrated that the recent Breakthrough Listen Initiative, and indeed many previous SETI radio surveys, place stronger limits on the prevalence of extraterrestrial intelligence in the distant Universe than is often fully appreciated.

Key words: extraterrestrial intelligence — astrobiology — radio continuum: galaxies — galaxies: active

1 INTRODUCTION

The Breakthrough Listen Initiative (Worden et al. 2017) is conducting the most thorough and comprehensive SETI (Search for Extraterrestrial Intelligence) programme ever conducted. The initiative greatly surpasses previous efforts in all regards but particularly in terms of spectral and temporal resolution, data processing techniques and compute capacity, observing time, raw sensitivity and human effort. The results of the initial first phase of observations have been published (Enriquez et al. 2017; Price et al. 2020; Gajjar et al. 2021; Traas et al. 2021; Franz et al. 2022) and the first signals of interest have also been identified and rigorously analysed (Sheikh et al. 2021; Smith et al. 2021). The longer term goal of the Breakthrough Listen Initiative over the next few years is to survey one million nearby stars, the entire Galactic plane, the galactic centre and a diverse range of 123 nearby galaxies located at distances of up to 30 Mpc.

The initial searches have focused on targeting stars in the Milky Way, in particular nearby systems. Recognising that these radio observations are typically also sensitive to many other cosmic objects in the radio telescope's natural field-of-view, Wlodarczyk-Sroka et al. (2020) extended the Breakthrough Listen (hereafter BL) surveys of 1327 stars targeted by Enriquez et al. (2017) and Price et al. (2020) to take into account other stellar objects in the field. In particular, stars

with parallaxes measured by *Gaia*, extended the sample from the original 1327 target stars to 288315 stellar objects, thus permitting Wlodarczyk-Sroka et al. (2020) to place much tighter limits on the prevalence of nearby extraterrestrial transmitters.

Most recently, Tremblay et al. (2022) have used the Murchison Widefield Array (MWA) at ∼ 150 MHz to perform a blind search of more that 3 million stars toward the Galactic Centre but with relatively course spectral resolution (∼ 10 kHz).

What is also not always fully appreciated is that radio SETI observations targeting nearby stars, have a field of view that naturally includes a great number and wide range of different background *extragalactic* systems. Indeed, this point is traditionally ignored in the analysis of SETI data. However, this fact is of significant interest because although extragalactic systems are located at distances that are many orders of magnitude larger than the nearest galactic stars, they contain hundreds of billions of stars, all simultaneously located within the main response of the radio telescope beam. Assuming these galaxies are not unlike our own Milky Way, a significant fraction of these stars may host planets located within the habitable zone (Batalha 2014). And while the luminosity function of extraterrestrial transmitters is currently unknown, it might not be too surprising if it was represented by a power-law suggesting that a population of rare

but very powerful sources might be observable at great distance (e.g. Drake et al. (1973)).

Gray & Mooley (2017) performed a very well motivated search of two nearby galaxies - M31 and M33 at a distance of 760 and 970 kpc respectively, using the JVLA. Multiple pointings were used in order to cover the full optical extent of both galaxies. Although the spectral resolution and bandwidth of this observation was relatively modest, the large number of stars observed simultaneously made this a rather pertinent search strategy - one that is very relevant to the work presented in this paper.

In a very welcome effort to expand the diversity of targets surveyed by the BL Initiative, Lacki et al. (2021) has compiled an additional catalogue of possible targets, with the ambition of including "one of everything" - a complete range of cosmic phenomena or astrophysical "exotica". The catalogue includes 816 distinct targets and is remarkably wide ranging, including minor bodies of the solar system, planetoids, giant planets, stars, collapsed objects, stellar groups, nebulae and the ISM, galaxies, active galactic nuclei (AGN), galaxy associations, and large-scale structures. In addition to comprising a large amount of baryonic matter in diverse configurations, this sample represents environments that may very well be preferred for technologically capable life that may be much more evolved than our own species and/or have evolved along exotic trajectories.
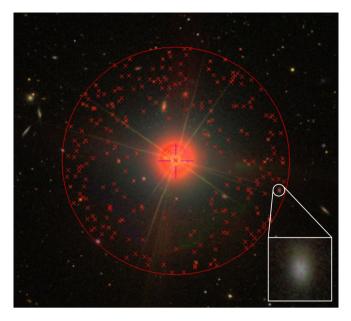
The main thrust of the research presented here is to consider the type of extragalactic objects (and indeed astrophysical exotica) that are routinely observed by SETI radio surveys that target nearby stars but unavoidably also include other background sources within the telescope's natural field of view. In this paper, an attempt has been made to assess the impact of this effect by making a study of a 469 field subset of the 692 fields first observed by Enriquez et al. (2017) using the 100-m Greenbank Telescope (GBT) at L-band. The form of the paper is as follows - in section 2 the field selection is considered and the approach used to identify extragalactic objects also described. Section 3 presents the main results, including some detailed examples of the exotica present in these fields. Section 4 uses these results to expand the parameter space explored by SETI surveys, and to place limits on the prevalence of very powerful extraterrestrial transmitters. Section 5 presents the overall conclusions of the paper. In what follows, a flat cosmology with $H_o = 70$ km/s/Mpc and $\Omega_M = 0.3$ is adopted.

2 FIELD SELECTION AND OBJECT IDENTIFICATION

2.1 Field Selection

In support of the BL observing programme, Isaacson et al. (2017) created an initial target list of 1709 nearby stars, including a range of different spectral type. The sample includes the 60 nearest stars (< 5 pc) with the remaining stars located within $5-50$ pc. Enriquez et al. (2017) observed 692 of these 1709 stars with the 100-m Greenbank Telescope (GBT) at 1.1-1.9 GHz.

Not surprisingly, many of the BL stars are also located near the galactic plane. These fields can be very crowded, and the chances of misidentifying galactic stars as extragalactic objects is significant. In order to reduce potential contamination by galactic sources, 92 fields were removed from the sample of 692 stars for which the target star was located within ±10 degrees of the galactic plane. Since the stars observed are typically nearby, many of them are also quite bright, especially in the optical. The very bright diffraction patterns associated with these stars makes it difficult to reliably identify other sources in the rest of the field. In order to alleviate this effect, stars

Figure 1. An optical SDSS9 colour image of the stellar field centred on BL J033901.1-053736.5, showing the extent of the FWHM for the GBT at L-band circled in red. The NED identifications in the field are represented by red crosses. The nearby galaxy, WISEA J033845.71-053842.1 is circled in the main image, with a close up view presented at the bottom right of the figure. The scale of the square inset is 15×15 arcseconds.

with $m_V < 5$ were identified and a further 120 fields were removed from the reduced sample. Finally, because many of the target stars are actually located in multiple stellar systems, 11 cases of overlapping fields were identified, and for each pair, one field was removed from the sample. This left a grand total of 469 fields in the final sample.

2.2 Object identification

Following Wlodarczyk-Sroka et al. (2020), the FWHM of the GBT at L-band was adopted to be 8.4 arcminutes. All object searches were therefore conducted employing cone searches with a radius of 4.2 arcminutes. At the edge of the cone, the sensitivity of the GBT is reduced by a factor of 2, compared to on-axis observations. It should therefore be noted that this radial cutoff is therefore somewhat arbitrary since the GBT retains some sensitivity beyond this point.

The NASA/IPAC Extragalactic Database (NED[1]) was used to search for objects within the central 4.2 arcminutes of each field. NED is the largest and most comprehensive online database of cosmic objects that lie beyond the Milky Way (Mazzarella 2020). For each of the 469 fields, a cone search of radius 4.2 arcminutes was performed. Some additional information on the fields was obtained by repeating the search on each field using SIMBAD[2] (Wenger et al. 2000). Extensive use of Aladin [3] (Bonnarel et al. 2000; Mazzarella 2020) was made to interrogate both the NED and SIMBAD data base servers, and to generate multi-wavelength images of each field. In particular, images were made for each field with Aladin via the DSS2, PanSTARSS DR1, SDSS9, 2MASS, GALEX, AllWISE, WENSS and NVSS survey collections. The Aladin Macro controller was used

---

[1] https://ned.ipac.caltech.edu/
[2] http://simbad.u-strasbg.fr/simbad/
[3] https://aladin.cds.unistra.fr/

to drive scripts that greatly reduced the administrative burden of executing these repetitive tasks on each of the 469 fields. It should be noted that the centre of each field was defined as the pointing position used by the GBT. Since some of the stars have large proper motions, the multi-wavelength images (typically made at a range of different epochs) often show the central star (or stellar system) offset from the centre of the field. Fig.1 presents a typical field.

3 RESULTS

A total of 143024 objects were identified by NED, including 17810 point sources, 28405 galaxies, 87841 Infrared sources, 44 QSOs, 8016 Ultraviolet sources, 401 X-ray sources, 398 radio sources, 11 Absorption line systems, 5 Gamma ray sources, 53 Galaxy cluster members, 33 galaxy groups, 6 galaxy pairs and 1 galaxy triple. For this sample, NED also reports spectroscopic redshifts for 989 objects and photometric redshifts for 434 objects. Clearly many of the objects fall into the category of "astrophysical exotica" as defined earlier by Lacki et al. (2021). In the following sub-sections, some examples of the wide range of various exotica are presented, with an emphasis on those systems that are relatively nearby and for which some constraints on the nature and prevalence of powerful transmitters may be inferred.

3.1 Selected exotica

3.1.1 Nearby galaxies

Visual inspection of the SDSS and DSS2 optical images of each field, reveals a significant number of extended, nearby galaxies contained within the 4.2 arcminute FWHM of the GBT. For sources identified by NED as ordinary galaxies, 6 are convincing examples of galaxy scale systems with $z < 0.02$. Table 1 presents the main properties of these systems. Fig.1 includes WISEA J033845.71-053842.1 - a galaxy located at $z = 0.010824$.

3.1.2 Interacting galaxies and star forming regions

The field BL J233623.1+020609.0 provides a good example of an interacting pair of galaxies - NGC 7714 at $z = 0.009333$ and NGC 7715 at $z = 0.009243$. NGC7714 (also known as Arp 284) is a prototypical starburst galaxy that is interacting with its smaller neighbour NGC 7715 - the average star formation rate is $\sim 1 M_\odot y^{-1}$ and its properties are comparable to M82 (see Lançon et al. (2001) and references therein). NGC 7714 is detected across the electromagnetic spectrum, and is also associated with NVSS J233614+020918, 2 supernova events (SN 1999dn & SN 2007fo) and 2 possible Ultra-luminous X-ray candidates. Located at a distance of ~ 40 Mpc this system is only a little further away than the BL galaxy sample's limit (< 30 Mpc). Fig.2 shows the field BL J233623.1+020609.0, containing NGC 7714 and NGC 7715.

3.1.3 Galaxy clusters

The presence of nearby galaxy clusters (and galaxy groups) is of special interest since it greatly increases the number of potential extraterrestrial transmitters simultaneously present within a single field of view, located at the same distance (see also section 4.2). The nearest galaxy cluster is located in the field BL J143328.4+525435.3 - there are eight galaxies with measured cluster redshifts in the GBT's

Figure 2. An optical PanSTARRS DR1 z and g broadband filters colour image of the stellar field centred on BL J233623.1+020609.0, showing the extent of the FWHM for the GBT at L-band circled in red. The interacting galaxies NGC 7714 and NGC 7715 are clearly labeled and are located close to the edge of 4.2 arcminute search cone.

4.2 arcminutes radial field of view - Table 2 presents the main properties of the cluster members.

Fig. 3 shows the field BL J143328.4+525435.3. It should be noted that this field also contains several AGN located at higher redshift.
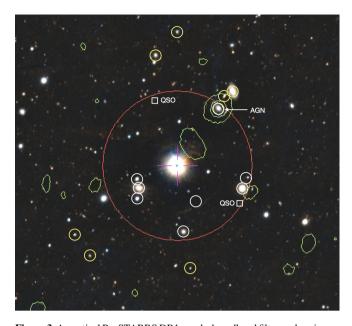
3.1.4 Nearby AGN

The nearest AGN identified by NED is WISEA J080816.59+210857.0 (also identified as SDSS J080816.59+210857.1) located at a redshift of $z = 0.142090$ in field BL J080812.8+210612.2. The source is included in the quasars and active nuclei catalogue of Véron-Cetty & Véron (2010). Oh et al. (2015) classify the source as a low-luminosity Type 1 AGN in which the central engine is viewed directly without significant obscuration.

3.1.5 Radio-loud galaxies

Somewhat ironically, a few of the BL fields contain relatively bright radio loud sources detected in various surveys, including NVSS (Condon et al. 1998) and WENSS (Rengelink et al. 1997). Prominent examples in our sample include: NVSS 132105+341502 and NVSS J194137+503431 (3C304). The main properties of NVSS 132105+341502 (see (Caccianiga et al. 2008) and Véron-Cetty & Véron (2010)) are presented in Table 3.

NVSS J194137+503431 is a radio source that straddles the 4.2 arcminute search cone of BL field J194148.6+503127.5, and is part of the very bright and extended radio source 3C402. 3C402 has an integrated flux density of $\sim 10.1 \pm 1.0$ Jy at 178MHz (Kellermann et al. 1969) and is associated with NVSS J194136+504017 (0.586 ± 0.019 Jy), NVSS J194146+503548 1.884 ± 0.058 Jy, and NVSS J194142+503750 0.489 ± 0.015 Jy, in addition to
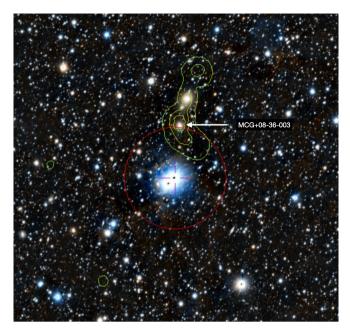
Figure 3. An optical PanSTARRS DR1 z and g broadband filters colour image of the stellar field centred on BL J143328.4+525435.3, showing the extent of the FWHM for the GBT at L-band circled in red. Members of the cluster located at $z \sim 0.046$ are identified with the white circles. Several prominent members of this cluster lying outside of the 4.2 arcminutes FWHM are also identified with yellow circles. Several AGN are also located within the search cone, including 2 QSOs (labelled) and MCG +09-24-014 which is an AGN.

Figure 4. An optical PanSTARRS DR1 z and g broadband filters colour image of the stellar field centred on J194148.6+503127.5, showing the extent of the FWHM for the GBT at L-band circled in red. A contour plot of 3C402 is superimposed upon the optical image. MCG+08-36-003 is identified in the figure, straddling the 4.2 arcminute search cone.

NVSS J194137+503431 0.151 ± 0.005 Jy. Fig.4 presents 3C402 superimposed upon a PanSTARRS optical image of the field BL J194148.6+503127.5. Recent highlights from the on-going VLASS survey, resolve 3C402 into at least two separate radio galaxies (Lacy et al. 2020). 3C402 (NVSS J194137+503431) is identified with a galaxy group - the details are presented in Table 4.

3.1.6 Gravitational lenses

One confirmed gravitational lens system is identified, MM184222+593828 (Lestrade et al. 2010), and one lens candidate, CFHTLS J020832.1-043315 (More et al. 2016). Our focus lies with the confirmed system since this also has a measured redshift. MM184222+593828 was first identified as a high redshift Sub-mm Galaxy using the MAMBO bolometer array at IRAM (Lestrade et al. 2010). Initially, extremely large lensed magnifications (μ) were implied ($\mu \sim 300$) in order to account for estimated IR luminosity of the system but radio observations by McKean et al. (2011) using the Westerbork Synthesis Radio Telescope (WSRT) at 1.4 GHz suggested much more modest values were required. VLA observations of CO (Lestrade et al. 2011) determined the redshift of the system to be $z = 3.93$ and revealed a complete Einstein ring with a diameter of 1.4 arcseconds. A revised estimate of the IR luminosity of the system by Lestrade et al. (2011), was consistent with the analysis of McKean et al. (2011), implying a lens magnification of $\mu \sim 12$ (Lestrade et al. 2011).

4 PLACING LIMITS ON THE PREVALENCE OF DISTANT EXTRATERRESTRIAL TRANSMITTERS

4.1 SETI survey figure of merit

Enriquez et al. (2017) first introduced the Continuous Waveform Transmitter Figure of Merit (CWTFM) for SETI surveys. The CWTFM reflects the likelihood of finding an extraterrestrial signal above a specific minimum Equivalent Isotropic Radiated Power (EIRP$_{min}$), such that:

$$\text{CWTFM} = \zeta_{AO} \, \frac{\text{EIRP}_{min}}{N_* \nu_{rel}}, \qquad (1)$$

where N_* is the total number of stars observed per pointing and the fractional bandwidth ν_{rel} is the total bandwidth of the receiver normalized by the central observing frequency, and ζ_{AO} is a normalising constant such that CWTFM is 1 for an EIRP equal to that of former Arecibo Planetary Radar system (10^{13}W). Smaller values for the CWTFM implies surveys that are more complete and/or have better sensitivity. For example, the initial survey of Enriquez et al. (2017) has a CWTFM ~ 0.85. Price et al. (2020) made a significant improvement on the results of Enriquez et al. (2017), by employing a larger range of Doppler drift rate (± 4 Hz s^{-1}) and lowering the SNR of the original analysis from 20 to > 10, and including more observations with GBT and Parkes radio telescopes at S-band, achieving a CWTFM of ~ 0.11. By including other galactic stars in the telescope's field of view, Wlodarczyk-Sroka et al. (2020) improved further upon Price's figure, obtaining a CWTFM of 0.04 for nearby stars. For comparison, the previous extragalactic search made by Gray & Mooley (2017) has a CWTFM of ~ 136.

Following Wlodarczyk-Sroka et al. (2020), the EIRP$_{min}$ obtained for distant objects in the field of view is estimated by scaling from the values already determined by Price et al. (2020) - at a distance of 50 pc, the EIRP$_{min}$ for the GBT at L-band is 2.1×10^{12} W. By adopt-

ing a Gaussian function for the telescope beam shape, the reduced response of the telescope at the position of the source is also taken into account. For simplicity, it is assumed that the galaxies considered here contain about the same number of stars (N_*) as the Milky Way, more specifically we add a level of uncertainty to this figure, assuming $N_* \sim 10^{11\pm0.3}$. We believe that this is a reasonable assumption - in particular, the objects used to derive the results presented later in Fig. 5, are all massive galaxies with absolute magnitudes that are comparable with or in excess of the Milky Way.

4.2 Results

Table 5 presents the CWTFM, EIRP$_{min}$ and Transmission Rate (TR) values for some of the astrophysical exotica discussed in the previous section. The results suggest that interesting figures of merit can be achieved for these systems, especially nearby galaxy groups and clusters - in these cases the very large number of stars that are simultaneously in the telescope field of view partially compensates for the loss in sensitivity (a larger EIRP$_{min}$). It's interesting to include the gravitational lens MM184222+593828 in this analysis because of the large source magnification factor (~ 12) but the EIRP$_{min}$ for this system remains extremely large.

Following Enriquez et al. (2017), Price et al. (2020) and Franz et al. (2022), a subset of the results presented here are compared with previous surveys - in particular, Fig. 5 plots the "transmission rate", TR, ($\frac{1}{N_* \nu_{rel}}$) against EIRP$_{min}$ for various surveys. Note that the error bars of this work (red symbols) are determined by the uncertainty in the value of N_* associated with the nearby galaxies and galaxy groups identified in the field - for clarity these are presented at the 2-sigma level. Inclusion of our results for the interacting pair NGC 7714/NGC 7715, the 3C402 galaxy group, and the nearby AGN WISEA J080816.59+210857.0 extend the parameter space into a new region of smaller transmission rates and larger EIRP$_{min}$. If extraterrestrial transmitters follow a power-law distribution as shown in Fig. 5, they are probably confined to a region below the line that is a best fit to the results of Wlodarczyk-Sroka et al. (2020) and the new analysis presented here. This region represents "terra incognita" for SETI studies and its full exploration requires surveys with better sensitivity and a wider field of view. Fig. 5 also shows two gaps in EIRP$_{min}$ coverage - the first is due to the physical distance between the most distant stars in the Milky Way and our nearest galactic neighbours, and the second is due to the physical distance that separates our nearest galactic neighbours and the more distant galaxies considered here ($z \sim 0.01 - 0.14$). Targeting nearby galaxy groups and clusters, could address the latter issue while going deeper with longer integration times, would seem to be another promising approach.

It may be wise to sound a note of caution at this point with respect to whether adopting a simple power-law distribution for extraterrestrial transmitters is appropriate. Astronomers, and in particular radio astronomers, are very familiar with power-laws that operate over many orders of magnitude but there is no evidence to suggest that the luminosity function for extraterrestrial transmitters will be similarly broad, especially on the scales considered here. Indeed while some authors have followed Drake et al. (1973) in assuming a simple power-law distribution for extraterrestrial transmitters (e.g. Gulkis (1984) and Lampton (2002)), others have rejected this assumption entirely, (e.g. Dreher (2004)), arguing that delta functions may be more appropriate for engineered technology. A less extreme approach would be to adopt more nuanced probability functions, such as the Pareto distribution but without knowing the scales on which the distribution flattens, their application is also limited for our purposes. Even if

a power-law is indeed appropriate, the slope could be significantly steeper than that shown in Fig. 5.

Since the BL observations have an integration time of typically 3×5 minutes per target field, these surveys and the implied prevalence of powerful transmitters only relates to high-duty cycle transmitters that are in prolonged and continuous operation. With this as a caveat, we note that Enriquez et al. (2017) and Price et al. (2020) find no evidence for 100% duty cycle transmitters in the original survey, and it is therefore also possible to place some limits on the prevalence of such transmitters at extragalactic distances.
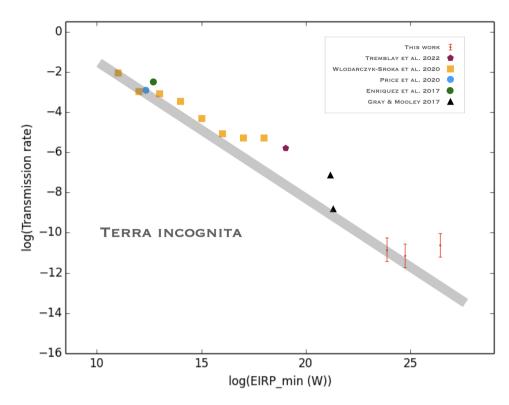
For example, in the case of NGC 7714 and 7715, no evidence is found for transmitters with an EIRP in excess of 7.5×10^{23} W. We define the prevalence of extraterrestrial transmitters as the fraction of stars in this interacting system that host a powerful (EIRP > 7.5×10^{23} W) long-duty cycle transmitter at the time the observations were made. For this particular system, the prevalence is $< 10^{-12}$.

We note that the gain of an antenna similar in scale to the Square Kilometre Array (SKA) is $\sim 10^8$, so the intrinsic transmitter power levels required are of order 10^{16} W, *i.e.* a total energy supply similar to that associated with a Kardashev Type I civilisation (Kardashev 1964) but only a tiny fraction of that available to a Type II civilisation ($\sim 10^{26}$ W). These power levels are many orders of magnitude greater than the most powerful radio transmitters routinely in use on Earth today ($EIRP \sim 10^{13}$ W), and it seems appropriate to consider whether such systems could be realised in practice. Currently, our most powerful radar systems combine together relatively modest transmitter powers with large phased arrays *e.g* Space Force. However, as noted earlier by Isaacson et al. (2017), there are no known physical laws that would preclude much larger EIRP figures to be attained and as receiver technology approaches the quantum noise limit, this is the only way to extend the range of many communication and radar applications. Benford et al. (2010) have considered favourably the feasibility of constructing messaging beacons operating at microwave frequencies with EIRPs approaching $\sim 10^{20}$ W using existing technology. These installations employ phased arrays of thousands of powerful transmitters distributed on scales of up to ~ 20 km^2 with the associated costs of construction estimated to be $\sim$ \$20 billion. Other sources of such powerful transmissions include operational installations *e.g.* microwave beamers for interstellar sails (Benford & Matloff 2019). It's difficult to predict what civilisations more advanced than our own might be capable of but surely it would not be too surprising if they employed much more powerful transmitters, assuming they routinely operate on interstellar scales.

5 SUMMARY

The current Breakthrough Listen programme, employing large single dish radio telescopes, also observes many other interesting sources in the field-of-view, in addition to the main target star. This paper has focused on the background sources that fill the field of view, including a wide range of varied astrophysical "exotica". These include nearby galaxies, galaxy groups, galaxy clusters, distant gravitational lens systems and a broad range of different AGN type. Extending the original BL analysis to take into account the potential response of extraterrestrial transmitters in these very distant systems, permits us to extend the parameter space explored by previous surveys and to place new constraints on the luminosity function of extraterrestrial transmitters, assuming the latter follow a simple power-law description.

Future work might choose to focus on regions of parameter space that represent SETI's "terra incognita" - suggesting that future sur-

Figure 5. A plot of the Transmission Rate against EIRP$_{min}$ for a range of SETI studies. The gray line is defined by the two most constraining values - this work (the results for NGC 7714/NGC 7715, the 3C402 galaxy group, and the nearby AGN WISEA J080816.59+210857.0) and that of Wlodarczyk-Sroka et al. (2020) - these data extend the parameter space into a new region of smaller transmission rates and larger EIRP$_{min}$. If extraterrestrial transmitters follow a power-law distribution, the region below this line represents a "terra incognita" for SETI surveys. The error bars of this work (red symbols) are presented at the 2-sigma level for clarity.

veys should consider: (i) going much deeper by employing longer integration times and/or more sensitive instruments (e.g. the SKA telescope now under construction) and (ii) targeting as large a number of potential targets simultaneously in a single pointing (e.g. nearby galaxies and galaxy groups/clusters). Combining these two approaches is another promising line of study e.g. long "stares" towards nearby groups and clusters. Finally, we note that SETI surveys that use beam-forming techniques to generate a limited number of relatively narrow pencil beams, will reduce the fraction of sky that is accessible to serendipitous discovery, as further detailed in Drake (2000). Employing interferometric techniques on antenna arrays that maintain the full field-of-view of the individual dishes would offer a better capability in this regard but at the price of significantly larger data volumes.

DATA AVAILABILITY

The data underlying this article are available in the article.

REFERENCES

Batalha N. M., 2014, Proceedings of the National Academy of Sciences, 111, 12647
Benford J., Matloff G., 2019, Journal of the British Interplanetary Society, 72, 51
Benford J., Benford G., Benford D., 2010, Astrobiology, 10, 475
Bonnarel F., et al., 2000, A&AS, 143, 33
Caccianiga A., et al., 2008, A&A, 477, 735
Condon J. J., Cotton W. D., Greisen E. W., Yin Q. F., Perley R. A., Taylor G. B., Broderick J. J., 1998, AJ, 115, 1693
Drake F., 2000, ATA Memo Series, 8, 1
Drake et al., 1973, in Sagan C., ed., , Communication With Extraterrestrial Intelligence. MIT press, p. 230
Dreher J. W., 2004, in Norris R., Stootman F., eds, Astronomical Society of the Pacific Conference Series Vol. 213, Bioastronomy 2002: Life Among the Stars. p. 467
Enriquez J. E., et al., 2017, ApJ, 849, 104
Franz N., et al., 2022, arXiv e-prints, p. arXiv:2201.00918
Gajjar V., et al., 2021, AJ, 162, 33
Gray R. H., Mooley K., 2017, AJ, 153, 110
Gulkis S., 1984, Telecommunications and Data Acquisition Progress Report, 77, 144
Isaacson H., et al., 2017, PASP, 129, 054501
Kardashev N. S., 1964, Soviet Ast., 8, 217
Kellermann K. I., Pauliny-Toth I. I. K., Williams P. J. S., 1969, ApJ, 157, 1
Lacki B. C., et al., 2021, ApJS, 257, 42

Lacy M., et al., 2020, PASP, 132, 035001

Lampton M., 2002, in Ekers R., Cullers J., Billingham J., Scheffer L., eds, , SETI 2020: A Roadmap for the Search of Extraterrestrial Intelligence. Mountain View: SETI press, p. 443

Lançon A., Goldader J. D., Leitherer C., González Delgado R. M., 2001, ApJ, 552, 150

Lestrade J. F., Combes F., Salomé P., Omont A., Bertoldi F., André P., Schneider N., 2010, A&A, 522, L4

Lestrade J.-F., Carilli C. L., Thanjavur K., Kneib J.-P., Riechers D. A., Bertoldi F., Walter F., Omont A., 2011, ApJ, 739, L30

Mazzarella J. M., 2020, in Pizzo R., Deul E. R., Mol J. D., de Plaa J., Verkouter H., eds, Astronomical Society of the Pacific Conference Series Vol. 527, Astronomical Data Analysis Software and Systems XXIX. p. 3

McKean J. P., Berciano Alba A., Volino F., Tudose V., Garrett M. A., Loenen A. F., Paragi Z., Wucknitz O., 2011, MNRAS, 414, L11

More A., et al., 2016, MNRAS, 455, 1191

Oh K., Yi S. K., Schawinski K., Koss M., Trakhtenbrot B., Soto K., 2015, ApJS, 219, 1

Price D. C., et al., 2020, AJ, 159, 86

Rengelink R. B., Tang Y., de Bruyn A. G., Miley G. K., Bremer M. N., Roettgering H. J. A., Bremer M. A. R., 1997, A&AS, 124, 259

Sheikh S. Z., et al., 2021, Nature Astronomy, 5, 1153

Smith S., et al., 2021, Nature Astronomy, 5, 1148

Traas R., et al., 2021, AJ, 161, 286

Tremblay C. D., Price D. C., Tingay S. J., 2022, arXiv e-prints, p. arXiv:2202.03324

Véron-Cetty M. P., Véron P., 2010, A&A, 518, A10

Wenger M., et al., 2000, A&AS, 143, 9

Wlodarczyk-Sroka B. S., Garrett M. A., Siemion A. P. V., 2020, MNRAS, 498, 5720

Worden S. P., et al., 2017, Acta Astronautica, 139, 98

Table 1: The properties of nearby galaxies contained within various BL fields (see section 3.1.1)

BL Field name	Source name	Type	z	Other ID
BL J033901.1-053736.5	WISEA J132337.71+291716.9	Starburst galaxy	0.013501	[SMB88] 2617
BL J132821.2-022143.9	WISEA J132814.15-021828.8	Galaxy	0.012270	2dFGRS TGN197Z212
BL J145622.9+493744.4	NGC 5797	Galaxy	0.013269	-
BL J153555.9+394952.0	IC 4563	Liner	0.014258	-
BL J153555.9+394952.0	NGC 5966	Galaxy Group	0.015048	-

Table 2: The main properties of the cluster members associated with BL J143328.4+525435.3 (see section 3.1.3)

Source name	Type	z	Other ID
WHL J143313.0+525748	galaxy	0.046300	-
DSS J143342.88+525346.9	galaxy	0.045790	-
WISEA J143343.08+525350.4	galaxy	0.045783	-
WISEA J143342.42+525320.3	galaxy	0.042923	-
DRS2017 000192	galaxy	0.045000	-
WISEA J143325.87+525053.5	galaxy	0.047088	-
BFW2006 20354	galaxy	0.046650	-
MCG +09-24-014	galaxy	0.047299	-

Table 3: The main properties of the radio source NVSS 132105+341502 (see section 3.1.5)

Source name	Type	z	$S_{1.4\ GHz}$ (mJy)	Size (")	Other ID
NVSS 132105+341502	Radio-loud AGN	0.452	474 ± 17	< 17	87GB 131847.5+343057 B2 1318+34B 6C B131847.2+343044 WISEA J132105.56+341500.9 2CXO J132105.4+341459

Table 4: Details of the galaxy group associated with 3C402 (see section 3.1.5)

Source name	Type	z	Other ID
MCG+08-36-003	galaxy	0.02595	CGCG 257-007
UGC 11465	galaxy	0.026061	-
WISEA J194140.93+503832.5	galaxy	0.027592	-
2MASX J19414453+5037151	galaxy	0.027805	-

Table 5: CWTFM and prevalence figures for extraterrestrial transmitters of astrophysical exotica

BL Field name	Source name	Type	d_l (Mpc)	Offset (')	Beam Response (%)	$EIRP_{min}$	N_*	logTR	CWTFM
BL J033901.1-053736.5	WISEA J033845.71-053842.1	Galaxy	46.7	3.98	53.6	9.8×10^{23}	$\sim 10^{11\pm0.3}$	-10.6 ± 0.3	919
BL J143328.4+525435.3	WHL J143313.0+525748 + others	Cluster	205.3	3.96	54.0	1.9×10^{25}	$\sim 10^{12\pm0.5}$	-11.6 ± 0.5	1781
BL J233623.1+020609.0	NGC 7714 & NGC 7715	Interacting system	40.3	3.88	55.3	7.5×10^{23}	$\sim 2 \times 10^{11\pm0.3}$	-10.9 ± 0.3	352
BL J080812.8+210612.2	WISEA J080816.59+210857.0	AGN	672.2	2.88	72.2	2.7×10^{26}	$\sim 10^{11\pm0.3}$	-10.6 ± 0.3	253125
BL J194148.6+503127.5	3C402 + others	Galaxy Group	113.4	4.2	50.0	5.4×10^{24}	$\sim 4 \times 10^{11\pm0.3}$	-11.2 ± 0.3	1265
BL J184244.0+593803.8	MM184222+593828	Lens system	35099.1	2.78	73.8	$7.6 \times 10^{29}\mu^{-1}$	$\sim 10^{11\pm0.3}$	-10.6 ± 0.3	$712500000\mu^{-1}$